

# UC Davis

## UC Davis Previously Published Works

### Title

Crystallographic and Compositional Dependence of Thermodynamic Stability of [Co(II), Cu(II), and Zn(II)] in 2-Methylimidazole-Containing Zeolitic Imidazolate Frameworks.

### Permalink

<https://escholarship.org/uc/item/6pz9c6pv>

### Journal

Chemistry of Materials, 35(17)

### ISSN

0897-4756

### Authors

Leonel, Gerson

Lennox, Cameron

Marrett, Joseph

et al.

### Publication Date

2023-09-12

### DOI

10.1021/acs.chemmater.3c01464

Peer reviewed

# Crystallographic and Compositional Dependence of Thermodynamic Stability of [Co(II), Cu(II), and Zn(II)] in 2-Methylimidazole-Containing Zeolitic Imidazolate Frameworks

Gerson J. Leonel, Cameron B. Lennox, Joseph M. Marrett, Tomislav Friščić,\* and Alexandra Navrotsky\*



Cite This: *Chem. Mater.* 2023, 35, 7189–7195



Read Online

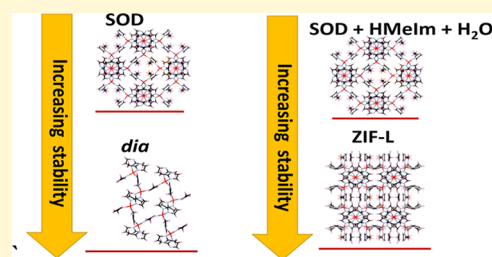
ACCESS |

Metrics & More

Article Recommendations

Supporting Information

**ABSTRACT:** We report the first systematic study experimentally investigating the effect of changes to the divalent metal node on the thermodynamic stability of three-dimensional (3D) and two-dimensional (2D) zeolitic imidazolate frameworks (ZIFs) based on 2-methylimidazolate linkers. In particular, the comparison of enthalpies of formation for materials based on cobalt, copper, and zinc suggests that the use of nodes with larger ionic radius metals leads to the stabilization of the porous sodalite topology with respect to the corresponding higher-density diamondoid (*dia*)-topology polymorphs. The stabilizing effect of metals is dependent on the framework topology and dimensionality. With previous works pointing to solvent-mediated transformation of 2D ZIF-L structures to their 3D analogues in the sodalite topology, thermodynamic measurements show that contrary to popular belief, the 2D frameworks are energetically stable, thus shedding light on the energetic landscape of these materials. Additionally, the calorimetric data confirm that a change in the dimensionality (3D → 2D) and the presence of structural water within the framework can stabilize structures by as much as 40 kJ·mol<sup>-1</sup>, making the formation of zinc-based ZIF-L material under such conditions thermodynamically preferred to the formation of both ZIF-8 and its dense, *dia*-topology polymorph.



## INTRODUCTION

Metal–organic frameworks (MOFs) have emerged over the last two decades as a promising class of advanced materials based on metal-containing nodes bridged through organic linkers, capable of forming two- (2D) and three-dimensional (3D) frameworks.<sup>1</sup> The linker–node assembly offers a high-degree of tunability,<sup>2–5</sup> providing access to potentially porous materials with a wide range of applications, from catalysis and gas sorption to rocket propellants.<sup>6–10</sup> A subclass of these materials are zeolitic imidazolate frameworks (ZIFs),<sup>6,7,11–15</sup> based on tetrahedrally coordinated metal nodes bridged through azolate linkers,<sup>11,16,17</sup> resulting in materials with analogous topologies as those found in natural zeolites.<sup>15</sup>

By employing different metal–ligand combinations,<sup>17,18</sup> a wide range of frameworks have been prepared with tunable material properties,<sup>19–21</sup> from sorption selectivity to material porosity.<sup>8,10,22</sup> Moreover, ZIFs and related composites also offer exceptional thermal and hydrothermal stability, including under acidic or basic conditions,<sup>23,24</sup> which is considered a prerequisite for any widespread application.<sup>25,26</sup> Furthermore, various ZIF polymorphs are accessible through variations of the synthesis conditions.<sup>18,27,28</sup> For example, real-time studies of the mechanochemical ball-milling preparation of ZIF-8, a popular ZIF material based on divalent zinc nodes and 2-methylimidazolate linkers (MeIm<sup>-</sup>), have revealed the sequential formation of the highly porous SOD-topology

material ZIF-8, followed by the appearance of katsenite (kat) and finally diamondoid (*dia*)-topology polymorphs.<sup>17,28,29</sup>

A considerable amount of effort has gone into investigating the synthesis of MOFs,<sup>18,29,30</sup> as well as the thermal stability<sup>31</sup> and resistance to structural degradation in water<sup>5</sup> of such materials, often with an emphasis on their kinetic stability.<sup>32</sup> Despite the focus on the kinetics of reactivity,<sup>32</sup> thermodynamic investigations are required to assess whether reactions can take place at all. To the best of our knowledge, the current explorations of the driving forces underlying MOF formation remain limited to a small number of systematic studies on the thermodynamic stability of MOFs, despite such understanding being critical to distinguishing between metastability and real stability, an important parameter for the adoption and development of MOFs in long-term applications. Recently, the thermodynamic stability of the MOF-74 family has been demonstrated to be directly related to their resistance to hydrolysis.<sup>33</sup> Our team has previously investigated the relationship between the linker substituent and the thermodynamic stability of isostructural ZIFs, suggesting that

Received: June 12, 2023

Revised: August 2, 2023

Published: August 21, 2023



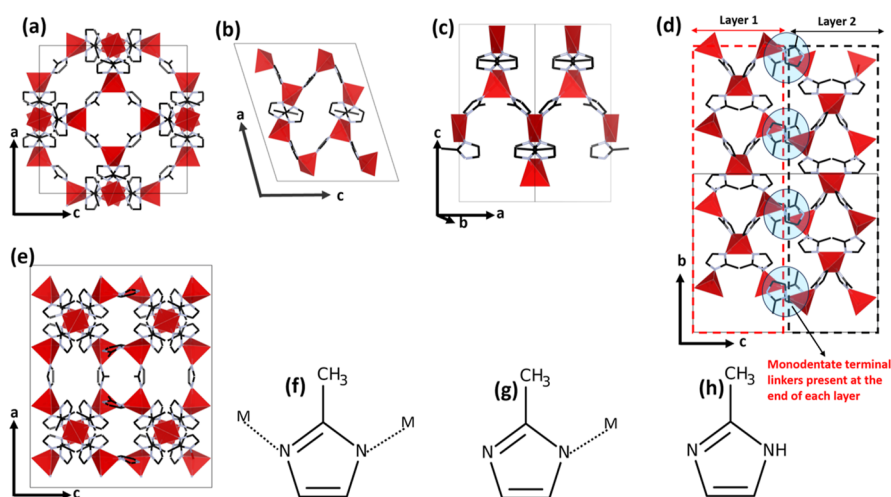


**Figure 1.** Structure of ZIFs in (a) 3D SOD topology, (b) 3D Zn and Co *dia*-topology, (c) 3D Cu *dia*-topology with distorted polyhedra, and (d,e) 2D ZIF-L configuration. All ZIFs contain (f) bidentate bridging linkers; however, ZIF-L has additional (g) terminal HMeIm and (h) free linkers between adjacent layers. Red tetrahedra represent metal (M(II)) centers. C–H bonds, water, and free linkers (in ZIF-L) are omitted for simplicity. Carbon and nitrogen are depicted in black and blue, respectively.

thermodynamic stability correlates with the electrostatic surface potential and Hammett  $\sigma$ -constants of the substituent.<sup>17</sup> The same study shows that variations in linker substituents of isostructural MOFs can cause the enthalpy of formation to change by as much as 30 kJ·mol<sup>-1</sup>.<sup>17</sup>

In this work, we present a complementary approach to assess ZIF stability, by investigating the stabilizing effect of metal substitution across a series of topologically similar frameworks. Rather than investigating the effect of linker substituents in isostructural ZIFs,<sup>17</sup> we investigate the enthalpic contribution of metal substitution on topologically similar ZIFs, namely, SOD-Co(MeIm)<sub>2</sub>,<sup>34</sup> SOD-Zn(MeIm)<sub>2</sub>,<sup>15</sup> *dia*-Co(MeIm)<sub>2</sub>,<sup>35</sup> *dia*-Cu(MeIm)<sub>2</sub>,<sup>36</sup> and *dia*-Zn(MeIm)<sub>2</sub>.<sup>35</sup> (Figure 1). This allows the direct assessment of the thermodynamic stability of these ZIFs. This systematic study enables better understanding of the stabilizing effects arising from the choice of metal nodes and what role framework topology has on metal effects. Furthermore, we expand on our work investigating 3D materials to include 2D layered systems Zn-ZIF-L<sup>37</sup> and Co-ZIF-L,<sup>38</sup> allowing us to capture the effect of framework dimension on thermodynamic stability.

## EXPERIMENTAL METHOD

Details of the synthetic procedure and characterization of the specimens are provided in the [Supporting Information](#).

**Thermodynamic Measurements.** A CSC 4400 isothermal microcalorimeter used for solution calorimetry was calibrated through the dissolution of KCl at 298.15 K. For calorimetric measurements and calculations, thermodynamic cycles (see the [Supporting Information](#)) were prepared for each of the ZIFs. For dissolution of the samples, 25 g of 5 N aqueous HCl solution was placed in a 50 mL Teflon cell under mechanical stirring at 0.5 Hz. The Teflon cell was inserted and contained inside the calorimeter maintained at 298.15 K. More details on the experimental procedure are provided in previous work.<sup>13</sup> The results we report show calculated statistical uncertainties within a 95% confidence interval.

## RESULTS AND DISCUSSION

The prepared ZIFs were analyzed by powder X-ray diffraction (PXRD), and the results confirm the formation of the desired frameworks (see the [Supporting Information](#)). Measured Fourier-transform infrared attenuated total reflectance

(FTIR-ATR) spectra (see the [Supporting Information](#)) indicate the presence of expected framework bonds. Thermogravimetric analysis (TGA) performed in air (see the [Supporting Information](#)) enabled the experimental evaluation of the metal content in the materials, with the final metal oxide residue formed during oxidative decomposition of the MOFs consistent with the expected chemical compositions.

**Thermodynamic Analysis.** Acid solution calorimetry permits quantitation of enthalpies of dissolution of each of the frameworks as well as the corresponding metal oxides and ligands. The use of enthalpies of dissolution and appropriate thermodynamic cycles (see the [Supporting Information](#)) enables determination of the enthalpic drive for the formation of each framework. To ensure that the heats of dissolution used for calculating heats of formation of the MOFs did not include enthalpic contributions resulting from the formation of cation coordination complexes from the interaction between the dissolved linker and the cation, separate experiments were conducted. The enthalpies associated with the individual dissolution of ~5 mg of CuO and 2-methylimidazole (HMeIm) in fresh HCl solution are  $-53.34 \pm 0.95$  and  $-43.56 \pm 0.26$  kJ·mol<sup>-1</sup>, respectively, based on four individual calorimetric runs for each material. The average enthalpy of dissolution for 5 mg of CuO in HCl solution containing ~5 mg of already dissolved HMeIm is  $-53.03 \pm 0.81$  kJ·mol<sup>-1</sup>. The average enthalpy of dissolution for 5 mg of HMeIm in HCl solution containing ~5 mg of already dissolved CuO is  $-43.75 \pm 0.59$  kJ·mol<sup>-1</sup>. It is concluded that no significant interaction occurs between the cations and linkers in the dissolved MOFs. The enthalpies of dissolution of the frameworks, linker, and corresponding metal oxide are summarized in [Table 1](#).

The heats of dissolution of all the metal oxides and linkers are exothermic ([Table 1](#)). Relative to end members (metal oxide and linker), the heats of formation of the 3D ZIFs are summarized in [Table 1](#). Examining the heat of formation in different dense-phase *dia*-topology ZIFs shows that the Co(II)-material is much more exothermic compared to both Zn- and Cu(II)-based analogues. Interestingly, the same trend is not observed for the corresponding porous SOD-topology polymorphs, wherein the heat of formation is more exothermic for the Zn-based ZIF-8 than for the Co(II)-based ZIF-67.<sup>40</sup> In

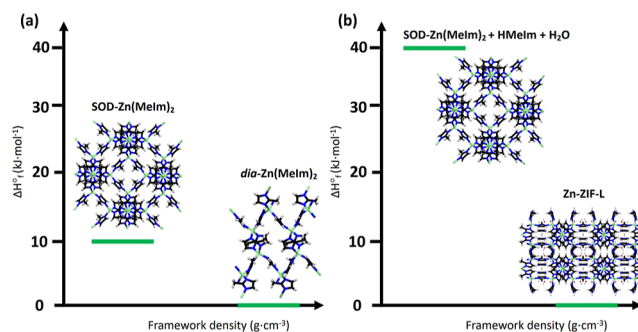
**Table 1. Enthalpies of Dissolution in 5 N HCl at 298.15 K and Formation from End Members (Metal Oxide, Linker, and Balance Water)**

sample	$\Delta H_{\text{dis}}$ (kJ·mol <sup>-1</sup> )	$\Delta H_f^\circ$ (kJ·mol <sup>-1</sup> )
HMeIm	-43.75 ± 0.59	
H <sub>2</sub> O <sup>28</sup>	-0.5	
CuO	-53.03 ± 0.81	
CoO <sup>39</sup>	-105.82 ± 0.36	
ZnO <sup>39</sup>	-72.29 ± 0.17	
<i>dia</i> -Co(MeIm) <sub>2</sub>	-146.81 ± 0.30	-46.01 ± 0.75
<i>dia</i> -Cu(MeIm) <sub>2</sub>	-126 ± 0.99	-14.03 ± 1.40
<i>dia</i> -Zn(MeIm) <sub>2</sub>	-127.86 ± 1.26	-31.43 ± 1.26
SOD-Co(MeIm) <sub>2</sub>	-177.5 ± 0.51	-15.32 ± 0.86
SOD-Zn(MeIm) <sub>2</sub>	-137.50 ± 0.94	-21.79 ± 0.94
Co-ZIF-L	-178.52 ± 0.32	-36.92 ± 0.76
Zn-ZIF-L	-120.29 ± 0.52	-61.62 ± 0.94

these systems, a more exothermic enthalpy of formation translates into overall greater thermodynamic stability with respect to hydrolysis, with the understanding that entropic effects are small. Consequently, the enthalpies of formation can be assumed to reflect the overall energetic landscape of these polymorphic systems. These results indicate that the stabilizing effect of different metals is highly dependent on the framework density, which is dictated by its topology (see Table 1).

Additionally, we use the enthalpies of reactions (1–4) (Table 2) to assess the thermodynamic stability of the 2D ZIF-L structures. The enthalpy of formation for the Co-ZIF-L and Zn-ZIF-L frameworks with respect to end members (metal oxide, linker, and water) is strongly exothermic by 37 and 62 kJ·mol<sup>-1</sup>, respectively. Similarly, both reactions (2) and (4) show that by starting from a 3D material with the open SOD topology as a reactant, the enthalpies for formation of Zn-ZIF-L and Co-ZIF-L are exothermic by 40 and 22 kJ·mol<sup>-1</sup>, respectively. These results suggest that if one considers the formation of the ZIF-L materials starting from the corresponding less dense SOD-topology frameworks in combination with an additional linker and water, the stabilizing effect arising from a change in the dimensionality from the 3D SOD-topology structure to the 2D ZIF-L material is comparable to and can be greater than that resulting from the formation of dense and more stable *dia*-polymorphs from the more porous, metastable SOD-topology ZIFs (see Figure 2).

Subsequently, we investigate different references for the assessment of stability in ZIF-L structures (see Table 2). The results in Table 2 highlight three main aspects of the thermodynamic stability of ZIF-L frameworks. First, the endothermic heat for reaction (4) [ $\Delta H_f^\circ$  (from *dia*)] shows that the replacement of SOD-Co(MeIm)<sub>2</sub> by *dia*-Co(MeIm)<sub>2</sub>

**Figure 2. Enthalpy diagrams for structures employing Zn(II) metal atoms as nodes, showing (a) higher metastability in SOD structures compared to *dia*-polymorphs and (b) higher enthalpy of SOD topology, water, and linker compared to Zn-ZIF-L analogues.**

as the reactant significantly disfavors the formation of Co-ZIF-L, thus indicating metastability of the 2D framework with increasing density of the 3D analogue in the Co(II) system. Surprisingly, a much smaller destabilization of Zn-ZIF-L frameworks is observed upon replacement of SOD-Zn(MeIm)<sub>2</sub> by the denser and more stable polymorph (*dia*-Zn(MeIm)<sub>2</sub>) as the reactant, hence the formation reaction (2) remains thermodynamically favorable (exothermic). This not only points to the discussed superior stability of Zn- and Co-ZIF-L structures compared to the respective SOD-topology ZIFs specimens but also indicates that in the presence of an additional linker and water, formation of the Zn-ZIF-L structure should even be preferred to the formation of the dense 3D *dia*-topology one. Although stabilization of a 2D structure over a denser 3D one can be seen as counterintuitive, we note that a recent report has established that the 2D layered polymorph of mercury(II) imidazolate should be more exothermic than its 3D quartz (qtz) topology analogue.<sup>41</sup>

Second, for reactions (2) and (4), the difference between  $\Delta H_f^\circ$  from *dia* and from SOD is directly related to the difference in the thermodynamic stability (enthalpy of formation) of the 3D polymorphs. Third, the high exothermic formation of Co-ZIF-L and Zn-ZIF-L from anhydrous 3D ZIFs and water suggests that the water in the structure is present as an actively participating stabilizing agent and not simply as a space-filling component. The addition of water and hydrogen bonding in the interlayer space may serve as a major source for the thermodynamic stability of 2D ZIF-L frameworks.

Previous reports have demonstrated that Zn-ZIF-L and Co-ZIF-L can undergo a solvent-mediated transformation into corresponding SOD-topology materials ZIF-8 and ZIF-67, respectively.<sup>37,38,42</sup> This may result from stabilization of sodalite structures by inclusion of other solvents. Typically,

**Table 2. Summary of Reactions Utilized for the Assessment of Enthalpic Changes Associated with the Formation of ZIF-L<sup>44</sup>**

reaction	$\Delta H_f^\circ$ (from end members)	$\Delta H_f^\circ$ (from <i>dia</i> )	$\Delta H_f^\circ$ (from SOD)
1. ZnO (s, 298.15 K) + 5/2 HMeIm (s, 298.15 K) + 1/2 H <sub>2</sub> O (l, 298.15 K) → Zn(MeIm) <sub>2</sub> (HMeIm) <sub>1/2</sub> (H <sub>2</sub> O) <sub>3/2</sub> (s, 298.15 K)	-61.62 ± 0.94		
2. Zn(MeIm) <sub>2</sub> (s, 298.15 K) + 1/2 HMeIm (s, 298.15 K) + 3/2 H <sub>2</sub> O (l, 298.15 K) → Zn(MeIm) <sub>2</sub> (HMeIm) <sub>1/2</sub> (H <sub>2</sub> O) <sub>3/2</sub> (s, 298.15 K)		-30.19 ± 1.33	-39.83 ± 1.14
3. CoO (s, 298.15 K) + 5/2 HMeIm (s, 298.15 K) + 1/2 H <sub>2</sub> O (l, 298.15 K) → Co(MeIm) <sub>2</sub> (HMeIm) <sub>1/2</sub> (H <sub>2</sub> O) <sub>3/2</sub> (s, 298.15 K)	-36.92 ± 0.76		
4. Co(MeIm) <sub>2</sub> (s, 298.15 K) + 1/2 HMeIm (s, 298.15 K) + 3/2 H <sub>2</sub> O (l, 298.15 K) → Co(MeIm) <sub>2</sub> (HMeIm) <sub>1/2</sub> (H <sub>2</sub> O) <sub>3/2</sub> (s, 298.15 K)		+9.08 ± 0.73	-21.60 ± 0.84

<sup>a</sup>All enthalpies are reported as kJ·mol<sup>-1</sup>.



the stability of a material is referred to as kinetic persistence to phase degradation, under a given set of conditions, even if allowed by thermodynamics, often without knowledge of the energetic drive for the reaction (i.e., true stability). Hence, the results of this work confirm the high thermodynamic stability of the 2D frameworks.<sup>43,44</sup> This expands the current knowledge of the energetic landscape in MOFs.

This study further permits the identification of various stabilization trends. For example, for materials with a SOD topology, Zn(II) containing materials are more stable than Co(II), and a similar observation is made for the 2D materials. However, for the close-packed *dia*-topology materials, the opposite trend is observed, with stability decreasing from Co(II) to Zn(II) and to Cu(II). In the SOD topology materials, there is an increase in thermodynamic stability of the framework with increasing ionic radius of the metal, with Zn(II) having the greatest stabilizing effect. However, in the *dia*-topology materials, smaller ionic radius nodes such as Co(II) seem to promote greater thermodynamic stability. These results suggest that the strength of organic and inorganic interactions is significantly dependent on the framework topology and dimensionality. The calculated enthalpies of formation further reveal that nodes consisting of larger ionic radius metals stabilize the porous SOD topology relative to the denser polymorphs in the *dia*-configuration.

It should be noted that the relative thermodynamic stability of materials with different substituents is determined by the respective bond strengths. In turn, these bond strengths are influenced by both the electronegativity and the ionic radius. Differences in electronegativity of the metal atom can lead to dissimilarities in metal–ligand bond length and/or strength,<sup>45,46</sup> resulting in different thermodynamic stabilization effects. For the metal substituents in this study, the electronegativity decreases from Cu to Co and to Zn, with specific values being 1.90, 1.88, and 1.65 on the Pauling scale.<sup>47–49</sup> Although the metal–ligand bond lengths in ZIF-8 and ZIF-67 are similar ( $\sim 2$  Å),<sup>50,51</sup> it is possible that Co(II) forms stronger bonds, which would be consistent with destabilization from lattice strain. Additionally, it is likely that an optimum bond distance exists that permits the favorable formation of shorter and/or stronger bonds while minimizing the lattice strain, in turn establishing a constraint on the electronegativity of metal atoms likely to stabilize frameworks dependent on topology.

Thermodynamic analysis of the *dia*-topology ZIFs reveals an increase in the stability of the structure with increasing electronegativity of the metal node upon substitution of Zn by Co(II). A further increase in electronegativity of the metal atom upon substitution of Co(II) by Cu(II), however, results in decreased stabilization relative to end members. The electronegativity of the atoms suggests that in the close-packed topology, there is only a minor decrease in the bond strength resulting from the substitution of Co(II) by Cu(II). These results could indicate an energetic penalty for lattice strain. Ultimately, in the *dia*-topology, metal atoms with electronegativity higher than  $\sim 1.88$  show less enthalpic stabilization relative to end members. Furthermore, Cu(II) atoms preferentially adopt a square-planar coordination, reflecting the Jahn–Teller effect.<sup>52–54</sup> The highly distorted tetrahedral coordination of Cu(II) in the herein explored *dia*-Cu(MeIm)<sub>2</sub> may contribute to the lower stabilizing effect of Cu(II) metal atoms, as seen in spinels.<sup>52–54</sup> In contrast, Zn(II) promotes the greatest stabilization in the SOD-topology as well

as in the ZIF-L systems. This is apparent, as the substitution of Zn(II) by Co(II) atoms decreases the thermodynamic drive for forming more porous frameworks. In this work, the stabilizing effect of metal nodes in SOD and ZIF-L frameworks decreases for metal atoms with electronegativity higher than  $\sim 1.65$ . This may suggest that compared to their denser analogues in the *dia*-topology, SOD and ZIF-L structures are more prone to destabilization resulting from lattice strain.

These observations point to a tradeoff between bond strength and lattice dynamics in framework materials such as ZIFs. Thermodynamically favorable configurations are expected to include strong bonds and reduced lattice strain. Such optimization of bonding can enable MOFs to be structurally flexible, allowing dynamic processes such as gate-opening.<sup>55–57</sup> It should be stressed that the electronegativity–stability relations we report, specifically the electronegativity values corresponding to thermodynamic penalty in the SOD- and *dia*-topology structures may be specific to the ZIFs and metals investigated herein. It is likely that electronegativity alone may not completely describe the energetic interplay in these materials, as the same topology-dependent electronegativity cut-off values may not apply to other MOF systems. Nevertheless, the trends seen here can serve as a starting point for identification and comparison of metal descriptors for increased stabilization across different reticular structures.

## CONCLUSIONS

This study provides a thermodynamic assessment of how different choices of the divalent metal node, from Co to Cu and Zn affect the thermodynamic stability of ZIF materials across both the more open SOD- and denser *dia*-topologies. Moreover, we also provide an experimental evaluation of the thermodynamic stability of 2D ZIF-L structures based on Co(II) and Zn nodes, compared to corresponding 3D *dia*- and SOD-topology framework materials. The results point to a possible optimum combination of bond strength and lattice strain to maximize the stability of the frameworks relative to end members. In the *dia*-topology, incorporation of metals with electronegativity higher than  $\sim 1.88$  decreases the thermodynamic drive for forming the framework. In the SOD-topology, the thermodynamic drive for forming the ZIF decreases upon the inclusion of metals with electronegativity higher than  $\sim 1.65$ . The presented thermodynamic analysis also reveals that the 2D ZIF-L structures possess high thermodynamic stability, which is likely to be enhanced by the presence of included water. As a result, the formation of Zn-ZIF-L and Co-ZIF-L structures is found to be thermodynamically driven with respect to popular 3D frameworks ZIF-8 and ZIF-67, respectively. Moreover, thermodynamic data also shows that the formation of Zn-ZIF-L should also be thermodynamically preferred, if an additional linker and water are accessible, to the formation of the dense *dia*-topology polymorph of ZIF-8. These results point to the importance of the effect of the metal, topology, and dimensionality (2D or 3D) on the design of thermodynamically more stable MOFs. The systematics observed in the energetics of formation in these materials provide an initial framework for the prediction and development of MOFs with greater thermodynamic stability and desired functionality.

## ■ ASSOCIATED CONTENT

## SI Supporting Information

The Supporting Information is available free of charge at <https://pubs.acs.org/doi/10.1021/acs.chemmater.3c01464>.

PXRD patterns, FTIR-ATR spectra, and TGA data, as well as detailed information about the synthesis of MOFs and other detailed experimental information (PDF)

## ■ AUTHOR INFORMATION

## Corresponding Authors

**Tomislav Friščić** – School of Chemistry Haworth Building, University of Birmingham, Birmingham B15 2TT, U.K.; Department of Chemistry, McGill University, Montreal QC H2L 0B7, Canada; [orcid.org/0000-0002-3921-7915](https://orcid.org/0000-0002-3921-7915); Email: [t.frisic@bham.ac.uk](mailto:t.frisic@bham.ac.uk)

**Alexandra Navrotsky** – School of Molecular Sciences and Center for Materials of the Universe, Arizona State University, Tempe, Arizona 85287, United States; Navrotsky Eyring Center for Materials of the Universe, School of Molecular Sciences and School of Engineering of Matter, Transport, and Energy, Arizona State University, Tempe, Arizona 85287, United States; [orcid.org/0000-0002-3260-0364](https://orcid.org/0000-0002-3260-0364); Email: [Alexandra.Navrotsky@ASU.edu](mailto:Alexandra.Navrotsky@ASU.edu)

## Authors

**Gerson J. Leonel** – Navrotsky Eyring Center for Materials of the Universe, School of Molecular Sciences and School of Engineering of Matter, Transport, and Energy, Arizona State University, Tempe, Arizona 85287, United States

**Cameron B. Lennox** – School of Chemistry Haworth Building, University of Birmingham, Birmingham B15 2TT, U.K.; Department of Chemistry, McGill University, Montreal QC H2L 0B7, Canada

**Joseph M. Marrett** – School of Chemistry Haworth Building, University of Birmingham, Birmingham B15 2TT, U.K.; Department of Chemistry, McGill University, Montreal QC H2L 0B7, Canada

Complete contact information is available at:

<https://pubs.acs.org/doi/10.1021/acs.chemmater.3c01464>

## Notes

The authors declare no competing financial interest.

## ■ ACKNOWLEDGMENTS

A.N. and G.L. acknowledge financial support from the National Science Foundation (NSF) Partnerships for International Research and Education (PIRE) grant #1743701. T.F., C.L., and J.M. thank the support of the NSERC Discovery Grant (RGPIN-2017-06467), NSERC John C. Polanyi award (JCP 562908-2022), Tier-1 Canada Research Chair Program (TF), NSERC CGS-D Scholarship (CL), Leverhulme International Professorship (TF), and the University of Birmingham.

## ■ REFERENCES

- (1) Yaghi, O. M. Reticular Chemistry: Molecular Precision in Infinite 2D and 3D. *Mol. Front. J.* **2019**, *03*, 66–83.
- (2) Kim, H.; Hong, C. S. MOF-74-Type Frameworks: Tunable Pore Environment and Functionality through Metal and Ligand Modification. *CrystEngComm* **2021**, *23*, 1377–1387.
- (3) Liu, J.; Zheng, J.; Barpaga, D.; Sabale, S.; Arey, B.; Derewinski, M. A.; McGrail, B. P.; Motkuri, R. K. A Tunable Bimetallic MOF-74

for Adsorption Chiller Applications. *Eur. J. Inorg. Chem.* **2018**, *2018*, 885–889.

(4) Wei, R.; Gaggioli, C. A.; Li, G.; Islamoglu, T.; Zhang, Z.; Yu, P.; Farha, O. K.; Cramer, C. J.; Gagliardi, L.; Yang, D.; Gates, B. C. Tuning the Properties of Zr6O8 Nodes in the Metal Organic Framework UiO-66 by Selection of Node-Bound Ligands and Linkers. *Chem. Mater.* **2019**, *31*, 1655–1663.

(5) Wade, C. R.; Corrales-Sanchez, T.; Narayan, T. C.; Dincă, M. Postsynthetic Tuning of Hydrophilicity in Pyrazolate MOFs to Modulate Water Adsorption Properties. *Energy Environ. Sci.* **2013**, *6*, 2172–2177.

(6) Titi, H. M.; Marrett, J. M.; Dayaker, G.; Arhangelskis, M.; Mottillo, C.; Morris, A. J.; Rachiero, G. P.; Friščić, T.; Rogers, R. D. Hypergolic Zeolitic Imidazolate Frameworks (ZIFs) as next-Generation Solid Fuels: Unlocking the Latent Energetic Behavior of ZIFs. *Sci. Adv.* **2019**, *5*, No. eaav9044.

(7) Titi, H. M.; Arhangelskis, M.; Katsenis, A. D.; Mottillo, C.; Ayoub, G.; Do, J.-L.; Fidelli, A. M.; Rogers, R. D.; Friščić, T. Metal–Organic Frameworks as Fuels for Advanced Applications: Evaluating and Modifying the Combustion Energy of Popular MOFs. *Chem. Mater.* **2019**, *31*, 4882–4888.

(8) Metzger, E. D.; Comito, R. J.; Wu, Z.; Zhang, G.; Dubey, R. C.; Xu, W.; Miller, J. T.; Dincă, M. Highly Selective Heterogeneous Ethylene Dimerization with a Scalable and Chemically Robust MOF Catalyst. *ACS Sustainable Chem. Eng.* **2019**, *7*, 6654–6661.

(9) Liu, J.; Goetjen, T. A.; Wang, Q.; Knapp, J. G.; Wasson, M. C.; Yang, Y.; Syed, Z. H.; Delferro, M.; Notestein, J. M.; Farha, O. K.; Hupp, J. T. MOF-Enabled Confinement and Related Effects for Chemical Catalyst Presentation and Utilization. *Chem. Soc. Rev.* **2022**, *51*, 1045–1097.

(10) Smoljan, C. S.; Li, Z.; Xie, H.; Setter, C. J.; Idrees, K. B.; Son, F. A.; Formalik, F.; Shafaie, S.; Islamoglu, T.; Macreadie, L. K.; Snurr, R. Q.; Farha, O. K. Engineering Metal–Organic Frameworks for Selective Separation of Hexane Isomers Using 3-Dimensional Linkers. *J. Am. Chem. Soc.* **2023**, *145*, 6434–6441.

(11) Wang, H.; Pei, X.; Kalmutzki, M. J.; Yang, J.; Yaghi, O. M. Large Cages of Zeolitic Imidazolate Frameworks. *Acc. Chem. Res.* **2022**, *55*, 707–721.

(12) Huang, X.-C.; Lin, Y.-Y.; Zhang, J.-P.; Chen, X.-M. Ligand-Directed Strategy for Zeolite-Type Metal–Organic Frameworks: Zinc(II) Imidazolates with Unusual Zeolitic Topologies. *Angew. Chem., Int. Ed.* **2006**, *45*, 1557–1559.

(13) Huang, X.; Zhang, J.; Chen, X. [Zn(Bim)<sub>2</sub>](H<sub>2</sub>O)<sub>1.67</sub>: A Metal–Organic Open-Framework with Sodalite Topology. *Chin. Sci. Bull.* **2003**, *48*, 1531–1534.

(14) Zhang, J.-P.; Zhang, Y.-B.; Lin, J.-B.; Chen, X.-M. Metal Azolate Frameworks: From Crystal Engineering to Functional Materials. *Chem. Rev.* **2012**, *112*, 1001–1033.

(15) Park, K. S.; Ni, Z.; Côté, A. P.; Choi, J. Y.; Huang, R.; Uribe-Romo, F. J.; Chae, H. K.; O’Keeffe, M.; Yaghi, O. M. Exceptional Chemical and Thermal Stability of Zeolitic Imidazolate Frameworks. *Proc. Natl. Acad. Sci. U.S.A.* **2006**, *103*, 10186–10191.

(16) Redfern, L. R.; Farha, O. K. Mechanical Properties of Metal–Organic Frameworks. *Chem. Sci.* **2019**, *10*, 10666–10679.

(17) Novendra, N.; Marrett, J. M.; Katsenis, A. D.; Titi, H. M.; Arhangelskis, M.; Friščić, T.; Navrotsky, A. Linker Substituents Control the Thermodynamic Stability in Metal–Organic Frameworks. *J. Am. Chem. Soc.* **2020**, *142*, 21720–21729.

(18) Lennox, B.; Do, J. L.; Crew, J. G.; Arhangelskis, M.; Titi, H. M.; Howarth, A. J.; Farha, O. K.; Friščić, T. Simplifying and Expanding the Scope of Boron Imidazolate Framework (BIF) Synthesis Using Mechanochemistry. *Chem. Sci.* **2021**, *12*, 14499–14506.

(19) Wang, J.; Kirlikovali, K. O.; Kim, S. Y.; Kim, D.-W.; Varma, R. S.; Jang, H. W.; Farha, O. K.; Shokouhimehr, M. Metal Organic Framework-Based Nanostructure Materials: Applications for Non-Lithium Ion Battery Electrodes. *CrystEngComm* **2022**, *24*, 2925–2947.

- (20) Pearson, A.; Bhagchandani, S.; Dinčá, M.; Johnson, J. A.; Johnson, J. A. Mixing Ligands to Enhance Gas Uptake in PolyMOFs. *Mol. Syst. Des. Eng.* **2023**, *8*, 591–597.
- (21) Zheng, Z.; Hanikel, N.; Lyu, H.; Yaghi, O. M. Broadly Tunable Atmospheric Water Harvesting in Multivariate Metal–Organic Frameworks. *J. Am. Chem. Soc.* **2022**, *144*, 22669–22675.
- (22) Luo, J.; Xu, H.; Liu, Y.; Zhao, Y.; Daemen, L. L.; Brown, C.; Timofeeva, T. V.; Ma, S.; Zhou, H.-C. Hydrogen Adsorption in a Highly Stable Porous Rare-Earth Metal–Organic Framework: Sorption Properties and Neutron Diffraction Studies. *J. Am. Chem. Soc.* **2008**, *130*, 9626–9627.
- (23) Gao, S.; Hou, J.; Deng, Z.; Wang, T.; Beyer, S.; Buzanich, A. G.; Richardson, J. J.; Rawal, A.; Seidel, R.; Zulkifli, M. Y.; Li, W.; Bennett, T. D.; Cheetham, A. K.; Liang, K.; Chen, V. Improving the Acidic Stability of Zeolitic Imidazolate Frameworks by Biofunctional Molecules. *Chem* **2019**, *5*, 1597–1608.
- (24) Yuan, S.; Feng, L.; Wang, K.; Pang, J.; Bosch, M.; Lollar, C.; Sun, Y.; Qin, J.; Yang, X.; Zhang, P.; Wang, Q.; Zou, L.; Zhang, Y.; Zhang, L.; Fang, Y.; Li, J.; Zhou, H.-C. Stable Metal–Organic Frameworks: Design, Synthesis, and Applications. *Adv. Mater.* **2018**, *30*, 1704303.
- (25) Kouser, S.; Hezam, A.; Khadri, M. J. N.; Khanum, S. A. A Review on Zeolite Imidazole Frameworks: Synthesis, Properties, and Applications. *J. Porous Mater.* **2022**, *29*, 663–681.
- (26) Mo, Z.; Tai, D.; Zhang, H.; Shahab, A. A Comprehensive Review on the Adsorption of Heavy Metals by Zeolite Imidazole Framework (ZIF-8) Based Nanocomposite in Water. *Chem. Eng. J.* **2022**, *443*, 136320.
- (27) Lewis, W.; Ruiz-Salvador, A. R.; Gómez, A.; Rodríguez-Albelo, L. M.; Coudert, F. X.; Slater, B.; Cheetham, A. K.; Mellot-Draznieks, C. Zeolitic Imidazole Frameworks: Structural and Energetics Trends Compared with Their Zeolite Analogues. *CrystEngComm* **2009**, *11*, 2272–2276.
- (28) Akimbekov, Z.; Katsenis, A. D.; Nagabhushana, G. P.; Ayoub, G.; Arhangelskis, M.; Morris, A. J.; Friščić, T.; Navrotsky, A. Experimental and Theoretical Evaluation of the Stability of True MOF Polymorphs Explains Their Mechanochemical Interconversions. *J. Am. Chem. Soc.* **2017**, *139*, 7952–7957.
- (29) Katsenis, A. D.; Puškarić, A.; Štrukil, V.; Mottillo, C.; Julien, P. A.; Užarević, K.; Pham, M.-H.; Do, T.-O.; Kimber, S. A. J.; Lazić, P.; Magdysyuk, O.; Dinnebier, R. E.; Halasz, I.; Friščić, T. In Situ X-Ray Diffraction Monitoring of a Mechanochemical Reaction Reveals a Unique Topology Metal–Organic Framework. *Nat. Commun.* **2015**, *6*, 6662.
- (30) Al Obeidli, A.; Ben Salah, H.; Al Murisi, M.; Sabouni, R. Recent Advancements in MOFs Synthesis and Their Green Applications. *Int. J. Hydrogen Energy* **2022**, *47*, 2561–2593.
- (31) Howarth, A. J.; Liu, Y.; Li, P.; Li, Z.; Wang, T. C.; Hupp, J. T.; Farha, O. K. Chemical, Thermal and Mechanical Stabilities of Metal–Organic Frameworks. *Nat. Rev. Mater.* **2016**, *1*, 15018–15115.
- (32) Rieth, A. J.; Wright, A. M.; Dinčá, M. Kinetic Stability of Metal–Organic Frameworks for Corrosive and Coordinating Gas Capture. *Nat. Rev. Mater.* **2019**, *4*, 708–725.
- (33) Voskanyan, A. A.; Goncharov, V. G.; Novendra, N.; Guo, X.; Navrotsky, A. Thermodynamics Drives the Stability of the MOF-74 Family in Water. *ACS Omega* **2020**, *5*, 13158–13163.
- (34) Saliba, D.; Ammar, M.; Rammal, M.; Al-Ghoul, M.; Hmadeh, M. Crystal Growth of ZIF-8, ZIF-67, and Their Mixed-Metal Derivatives. *J. Am. Chem. Soc.* **2018**, *140*, 1812–1823.
- (35) Shi, Q.; Chen, Z.; Song, Z.; Li, J.; Dong, J. Synthesis of ZIF-8 and ZIF-67 by Steam-Assisted Conversion and an Investigation of Their Tribological Behaviors. *Angew. Chem., Int. Ed.* **2011**, *50*, 672–675.
- (36) Xu, Y.; Marrett, J. M.; Titi, H. M.; Darby, J. P.; Morris, A. J.; Friščić, T.; Arhangelskis, M. Experimentally Validated Ab Initio Crystal Structure Prediction of Novel Metal–Organic Framework Materials. *J. Am. Chem. Soc.* **2023**, *145*, 3515–3525.
- (37) Deacon, A.; Briquet, L.; Malankowska, M.; Massingberd-Mundy, F.; Rudić, S.; Hyde, T. L.; Cavaye, H.; Coronas, J.; Poulston, S.; Johnson, T. Understanding the ZIF-L to ZIF-8 Transformation from Fundamentals to Fully Costed Kilogram-Scale Production. *Commun. Chem.* **2022**, *5*, 18.
- (38) Zhang, J.; Zhang, T.; Yu, D.; Xiao, K.; Hong, Y. Transition from ZIF-L-Co to ZIF-67: A New Insight into the Structural Evolution of Zeolitic Imidazolate Frameworks (ZIFs) in Aqueous Systems. *CrystEngComm* **2015**, *17*, 8212–8215.
- (39) Hughes, J. T.; Bennett, T. D.; Cheetham, A. K.; Navrotsky, A. Thermochemistry of Zeolitic Imidazolate Frameworks of Varying Porosity. *J. Am. Chem. Soc.* **2013**, *135*, 598–601.
- (40) Xu, W.; Chen, H.; Jie, K.; Yang, Z.; Li, T.; Dai, S. Entropy-Driven Mechanochemical Synthesis of Polymetallic Zeolitic Imidazolate Frameworks for CO<sub>2</sub> Fixation. *Angew. Chem., Int. Ed.* **2019**, *58*, 5018.
- (41) Speight, I. R.; Huskić, I.; Arhangelskis, M.; Titi, H. M.; Stein, R. S.; Hanusa, T. P.; Friščić, T. Disappearing Polymorphs in Metal–Organic Framework Chemistry: Unexpected Stabilization of a Layered Polymorph over an Interpenetrated Three-Dimensional Structure in Mercury Imidazolate. *Chem.—Eur. J.* **2020**, *26*, 1811–1818.
- (42) Fu, H.; Wang, Z.; Wang, X.; Wang, P.; Wang, C.-C. Formation Mechanism of Rod-like ZIF-L and Fast Phase Transformation from ZIF-L to ZIF-8 with Morphology Changes Controlled by Polyvinylpyrrolidone and Ethanol. *CrystEngComm* **2018**, *20*, 1473–1477.
- (43) Lee, S.; Oh, S.; Oh, M. Atypical Hybrid Metal–Organic Frameworks (MOFs): A Combinative Process for MOF-on-MOF Growth, Etching, and Structure Transformation. *Angew. Chem., Int. Ed.* **2020**, *59*, 1327–1333.
- (44) Low, Z.-X.; Yao, J.; Liu, Q.; He, M.; Wang, Z.; Suresh, A. K.; Bellare, J.; Wang, H. Crystal Transformation in Zeolitic-Imidazolate Framework. *Cryst. Growth Des.* **2014**, *14*, 6589–6598.
- (45) Cheng, C.-C.; Cheng, P.-Y.; Huang, C.-L.; Senthil Raja, D.; Wu, Y.-J.; Lu, S.-Y. Gold Nanocrystal Decorated Trimetallic Metal Organic Frameworks as High Performance Electrocatalysts for Oxygen Evolution Reaction. *Appl. Catal., B* **2021**, *286*, 119916.
- (46) Gao, K.; Guo, X.; Zheng, B.; Wang, J.; Wang, L. Investigation of Interface Compatibility in Stiff Polymer/Metal–Organic Frameworks. *Mater. Today Chem.* **2021**, *20*, 100458.
- (47) Hartmann, M. J.; Häkkinen, H.; Millstone, J. E.; Lambrecht, D. S. Impacts of Copper Position on the Electronic Structure of [Au<sub>25</sub>-XCu<sub>x</sub>(SH)<sub>18</sub>]– Nanoclusters. *J. Phys. Chem. C* **2015**, *119*, 8290–8298.
- (48) Hao, J.; Zhuang, Z.; Cao, K.; Gao, G.; Wang, C.; Lai, F.; Lu, S.; Ma, P.; Dong, W.; Liu, T.; Du, M.; Zhu, H. Unraveling the Electronegativity-Dominated Intermediate Adsorption on High-Entropy Alloy Electrocatalysts. *Nat. Commun.* **2022**, *13*, 2662.
- (49) Kamdar, M. H. The Occurrence of Liquid-Metal Embrittlement. *Phys. Status Solidi A* **1971**, *4*, 225–233.
- (50) Timofeeva, M. N.; Lukoyanov, I. A.; Panchenko, V. N.; Shefer, K. I.; Mel'gunov, M. S.; Bhadra, B. N.; Jhung, S. H. Tuning the Catalytic Properties for Cycloaddition of CO<sub>2</sub> to Propylene Oxide on Zeolitic-Imidazolate Frameworks through Variation of Structure and Chemical Composition. *Mol. Catal.* **2022**, *529*, 112530.
- (51) Zareba, J. K.; Nyk, M.; Samoć, M. Co/ZIF-8 Heterometallic Nanoparticles: Control of Nanocrystal Size and Properties by a Mixed-Metal Approach. *Cryst. Growth Des.* **2016**, *16*, 6419–6425.
- (52) Sahu, S. K.; Navrotsky, A. Thermodynamics of Copper-Manganese and Copper-Iron Spinel Solid Solutions. *J. Am. Ceram. Soc.* **2017**, *100*, 3684–3692.
- (53) Fu, L.; Yang, H.; Hu, Y.; Wu, D.; Navrotsky, A. Tailoring Mesoporous  $\gamma$ -Al<sub>2</sub>O<sub>3</sub> Properties by Transition Metal Doping: A Combined Experimental and Computational Study. *Chem. Mater.* **2017**, *29*, 1338–1349.
- (54) Shivaramaiah, R.; Tallapragada, S.; Nagabhushana, G. P.; Navrotsky, A. Synthesis and Thermodynamics of Transition Metal Oxide Based Sodium Ion Cathode Materials. *J. Solid State Chem.* **2019**, *280*, 121011.
- (55) Casco, E.; Cheng, Y. Q.; Daemen, L. L.; Fairen-Jimenez, D.; Ramos-Fernández, E. V.; Ramirez-Cuesta, A. J.; Silvestre-Albero, J. J.

Ramos-Fernández, E. V.; Ramirez-Cuesta, A. J.; Silvestre-Albero, J. Gate-opening effect in ZIF-8: the first experimental proof using inelastic neutron scattering. *Chem. Commun.* **2016**, *52*, 3639–3642.

(56) Krokidas, P.; Castier, M.; Moncho, S.; Sredojevic, D. N.; Brothers, E. N.; Kwon, H. T.; Jeong, H.-K.; Lee, J. S.; Economou, I. G. ZIF-67 Framework: A Promising New Candidate for Propylene/Propane Separation. Experimental Data and Molecular Simulations. *J. Phys. Chem. C* **2016**, *120*, 8116–8124.

(57) Nijem, N.; Wu, H.; Canepa, P.; Marti, A.; Balkus, K. J., Jr.; Thonhauser, T.; Li, J.; Chabal, Y. J. Tuning the Gate Opening Pressure of Metal–Organic Frameworks (MOFs) for the Selective Separation of Hydrocarbons. *J. Am. Chem. Soc.* **2012**, *134*, 15201–15204.